Circular waves on a stationary disk in rotating flow

Ö. Sava

Citation: Physics of Fluids (1958-1988) **26**, 3445 (1983); doi: 10.1063/1.864124
View online: http://dx.doi.org/10.1063/1.864124
View Table of Contents: http://scitation.aip.org/content/aip/journal/pof1/26/12?ver=pdfcov
Published by the AIP Publishing

LETTERS

The purpose of this Letters section is to provide rapid dissemination of important new results in the fields regularly covered by The Physics of Fluids. Results of extended research should not be presented as a series of letters in place of comprehensive articles. Letters cannot exceed three printed pages in length, including space allowed for title, figures, tables, references and an abstract limited to about 100 words.

Circular waves on a stationary disk in rotating flow

Ö. Savaş
School of Aerospace, Mechanical and Nuclear Engineering, University of Oklahoma, Norman, Oklahoma 73019

(Received 1 August 1983; accepted 26 September 1983)

Circular waves of a new type are observed in the disk boundary layer occurring on the end of a cylindrical cavity during impulsive spindown to rest. These waves occur around $z(\Omega_i/\nu)^{1/2}\approx 3.6$ and are reminiscent of Tollmien–Schlichting waves of an ordinary boundary layer. It is concluded that these waves are manifestations of the instabilities excited in the Bödewadt-type boundary layer developed over the disk.

Solutions of the boundary layer flows over a rotating disk in a rotating flow have been provided when both the disk and the fluid over it are rotating in the same direction.[1,2,3] The range extends from flow over a rotating disk (Kármán flow) to rotating flow over a stationary disk (Bödewadt flow). The velocity profiles exhibit numerous oscillations across the boundary layer which are prone to various modes of instabilities. Two such modes, both spiral, commonly known as type I and type II waves, were investigated by Gregory *et al.*,[4] Faller,[5] Faller and Kaylor,[6] and Tatro and Mollo-Christensen.[7] The nature of these flows is being investigated further, and our understanding is ever expanding. A new type of wave observed in a Bödewadt-type boundary layer is reported here. These waves are circular and continuing experiments indicate that these waves are not confined to the Bödewadt-type boundary layers only.

The experimental setup consists of a cylinder mounted on a programmable turntable (Fig. 1). The cylinder has an internal diameter $2R$ of 21.48 cm. The height-to-diameter ratio ($H/2R$) is 1.00. A Plexiglas top and an aluminum bottom are screwed onto two aluminum flanges which are fitted and glued onto the cylinder. The working fluid is water at 23°C (kinematic viscosity $\nu = 0.0094$ cm^2/sec). Aluminum flakes of approximately 40 μm diameter are used as visualization agents. The concentration is about 5×10^{-4} by weight which allows a visible depth of about 10 mm. To prevent the aluminum flakes from sticking to the walls, thus obscuring the view, the walls are coated with a very thin film of either a spray lubricant or a silicone grease. With this scheme one can see deeper into the flow, thereby making possible the photographs presented here. A Plexiglas insert is suspended from the top plate in order to have visual access into the disk boundary layer for cross-sectional visualizations. This reduces the cavity height to $0.75H$. The aluminum flake concentration is also decreased to about 10^{-5} to allow light penetration across the cylinder. The cylinder assembly is mounted on a turntable driven by a progammable servo amplifier. Constant speeds could be achieved within 0.1% of the set speed. Impulsive spindown to rest commands are implemented for the present experiments. The turntable assembly decelerates at a rate of 55 rad/sec^2 with negligibly small overshoot. These speed commands are used to mark time $t = 0$ and to trigger a digital counter whose display is photographed to record the time. After trying numerous illumination schemes, room lighting is found to be a suitable light source. Ideal lighting for plan view visualizations would be either a ring light source or a luminous ceil-

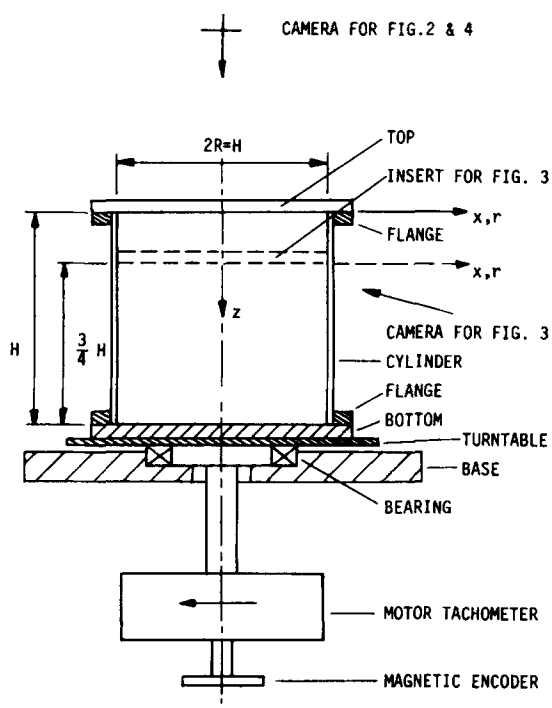

FIG. 1. Experimental setup and the reference system.

 0031-9171/83/123445-04$01.90

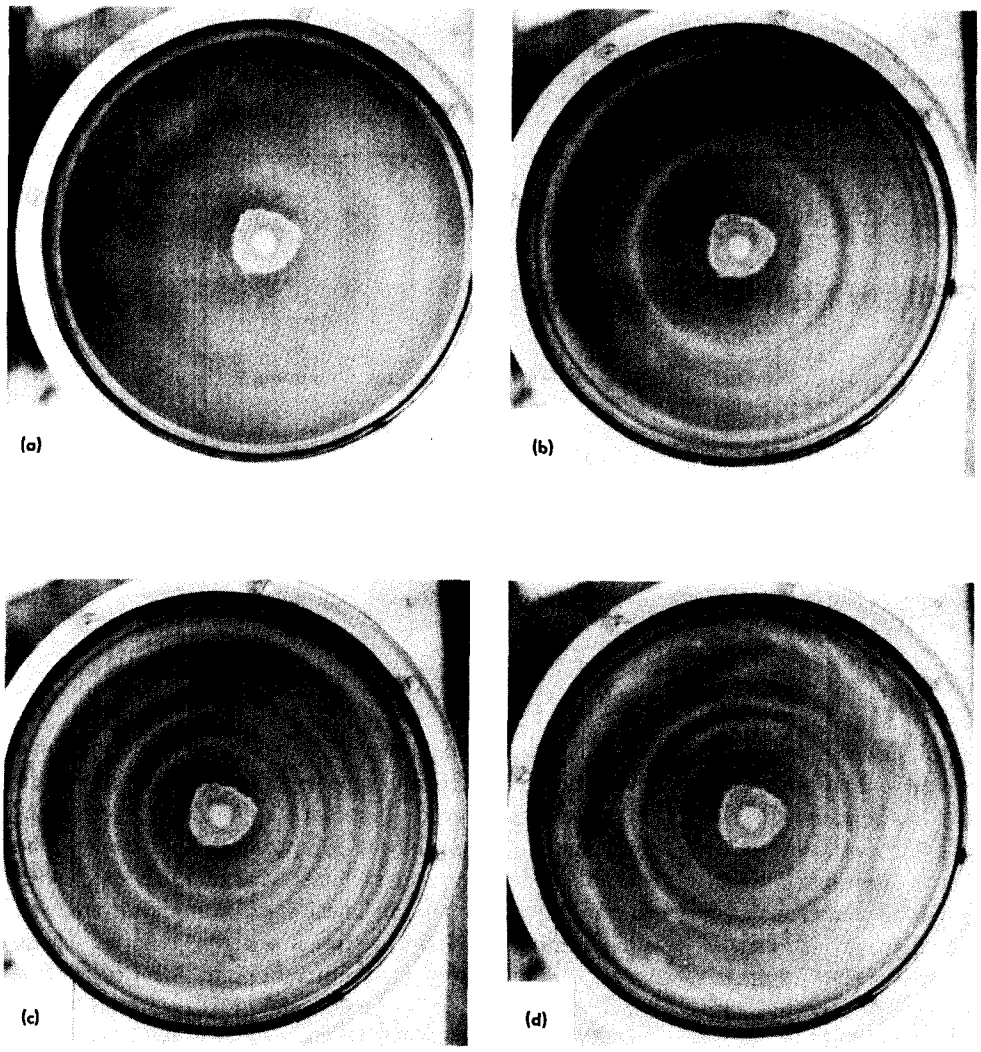

FIG. 2. Waves in the disk boundary layer during spindown to rest from $\Omega_i = 0.785$ rad/sec. Clockwise rotation. (a) $t = 3.4$ sec, $\Omega_i t = 2.7$ rad; (b) $t = 5.0$ sec, $\Omega_i t = 3.9$ rad; (c) $t = 6.3$ sec, $\Omega_i t = 5.0$ rad; and (d) $t = 8.4$ sec, $\Omega_i t = 6.6$ rad.

ing. A 1 mm sheet of laser light from a 2 W Argon-Ion laser is used for cross-sectional visualizations. Eight millimeter motion pictures are taken from the plan view.

Figures 2–4 show the waves in the disk boundary layer during impulsive spindown to rest. Figure 2 displays plan views of four successive stages of one realization of the flow. The cylinder and its contents had been rotating at a constant initial angular velocity $\Omega_i = 0.785$ rad/sec. Circular waves become visible after about 3 sec as shown in Fig. 2(a). Following the solution of the evolution of Kármán flow over a rotating disk, a few radians of rotation would be enough to establish a quasisteady boundary layer on the disk.[8,9] Assuming that the core is still rotating as a solid body with the initial angular velocity, then it must have traveled about 2.7 radians or 0.4 revolution. The disk boundary layer of the Bödewadt type must have had enough time to form, and the circular waves are then evolving in a developed boundary layer. By the time of Fig. 2(b), the waves are very distinct and are moving towards the center of the disk. The phase velocity is estimated from the pictures and the movies as 1.3 cm/sec with a slight decrease towards the center. The asymmetry in shading is due to the asymmetric locations of the ceiling lights with respect to the cylinder. The sharp contrast between the bright and dark regions indicates that the material surfaces are rolling up into azimuthal vortices. Observations in the cross-sectional view confirm the existence of these vortices (Fig. 3). The turbulent regions that first appear around the outer edges of the disk [Fig. 2(c)] originate from the fluid convecting from the cylinder side wall layer as this fluid undergoes an unstable motion [Fig. 3(d)]. This turbulent fluid eventually fills up the disk layer, and the regularity of the circular waves is lost. The last frame of Fig. 2 depicts the final phases of the flow.

The cross-sectional views of the boundary layer are shown in Fig. 3. The interior is visible up to radius $r/R \approx 0.8$, and on a distorted scale due to the lens effect of the cylinder. The initial rotation rate Ω_i is 0.785 rad/sec. Even though the aspect ratio is 0.75, the disk boundary layer is similar to that of Fig. 2. The orientation of the aluminum flakes render the boundary layer and fluid leaving it darker than the fluid in the core of the cylinder, thus making the initial phase of the waves hard to observe [Fig. 2(a) versus Fig. 3(b)]. As the waves develop, the material surfaces roll up into azimuthal vortices in the boundary layer. The cores of these vortices become visible as light regions in the dark boundary layer as seen in Figs. 3(c) and 3(d). Figure 3(e) is a summary of the observations in the cross-sectional view. The waves originate and roll into vortices around $z = 4$ mm or $z(\Omega_i/\nu)^{1/2} \approx 3.6$,

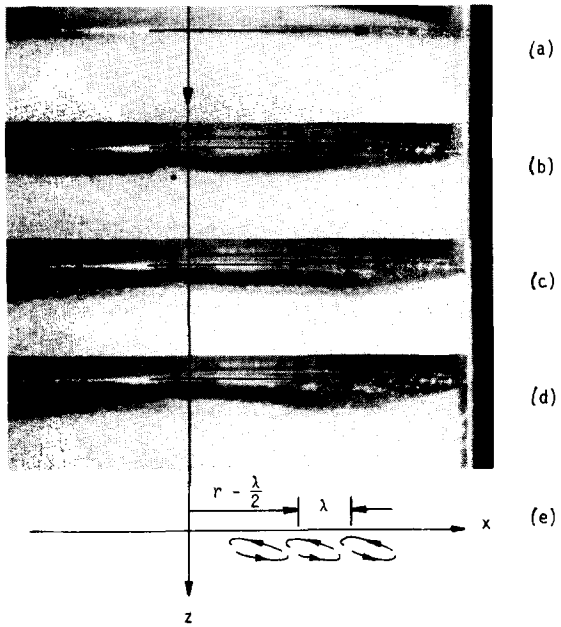

FIG. 3. Cross-sectional view of the disk boundary layer. $\Omega_i = 0.785$ rad/sec. Optical arrangement reveals the detail for $x > 0$ only. Note the turbulent fluid convecting from the side wall of the cylinder. (a) $t = 0$, reference system; (b) $t = 3.3$ sec, $\Omega_i t = 2.6$ rad; (c) $t = 5.1$ sec, $\Omega_i t = 4.0$ rad; (d) $t = 7.0$ sec, $\Omega_i t = 5.5$ rad; and (e) the summary and symbol definitions for Fig. 5.

which corresponds to the region where the radial flow of the Bödewadt boundary layer reverses direction and flows radially outward. The thickness to length ratio of the vortices is around 1/4.

The photographs of Fig. 4 depict the nature of the boundary layer at two higher initial rotation rates of the cylinder assembly. The most interesting picture is Fig. 4(a). Both circular waves and spiral waves are observed. The spiral waves have an angle of about 15° with respect to the tangential flow. They are evidently type I (class B) waves. The circular waves are no longer visible in Fig. 4(b). The view is filled with type I waves. They are itermittently broken, probably by type II waves (class A). At this high rotation rate, however, the deceleration time of the cylinder assembly becomes comparable to the evolution times of the boundary

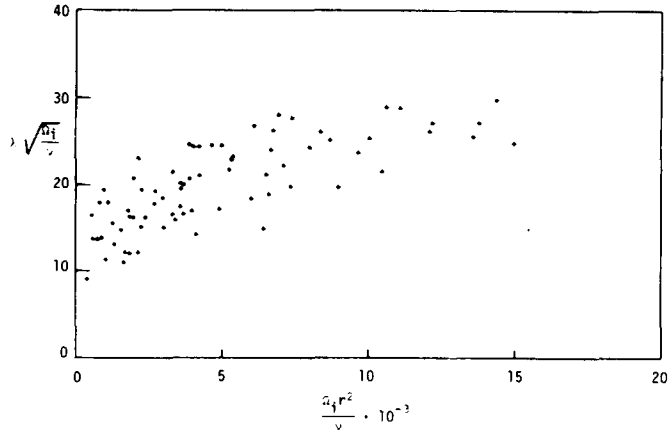

FIG. 5. Wavelengths of circular waves versus the local Reynolds number.

layer and the waves, and this picture must be interpreted with caution.

Figure 5 shows the wavelength λ of the observed cycles versus the local Reynolds number $\Omega_i r^2/\nu$ [see Fig. 3(e) for the definitions of λ and r]. The wavelength is scaled with the axial length scale $(\nu/\Omega_i)^{1/2}$ of the Bödewadt problem. The data of the figures are obtained from the analysis of numerous pictures. The ranges of λ, r, and Ω_i are 1.09–2.40 cm, 3.20–7.08 cm, and 0.628–3.14 rad/sec, respectively. Even though a functional relationship is clear, the scattering is too large to warrant a meaningfully fitted curve. Part of the scattering is due to the crude nature of manual data extraction from the pictures. A substantial part of the scattering, however, reflects the radial dependence of λ. Lastly, when the waves roll into vortices and slide on top of each other [cf. Fig. 3(e)], the observed cycle length is shorter than that of the unrolled wave [Fig. 2(a) versus Figs. 2(c) and 3]. The wavelengths are much smaller than 28δ of those of type II waves [δ is the boundary layer thickness, $\approx 6(\nu/\Omega_i)^{1/2}$ from Ref. 1 or ≈ 6 mm from Fig. 3]. The higher values of $\lambda\,(\Omega_i/\nu)^{1/2}$ in the figure correspond to the initial phase of the waves while the lower values correspond to the azimuthal vortices. An upper envelope to the data points, therefore, should represent the wavelength of the linear waves as a function of the local Reynolds number.

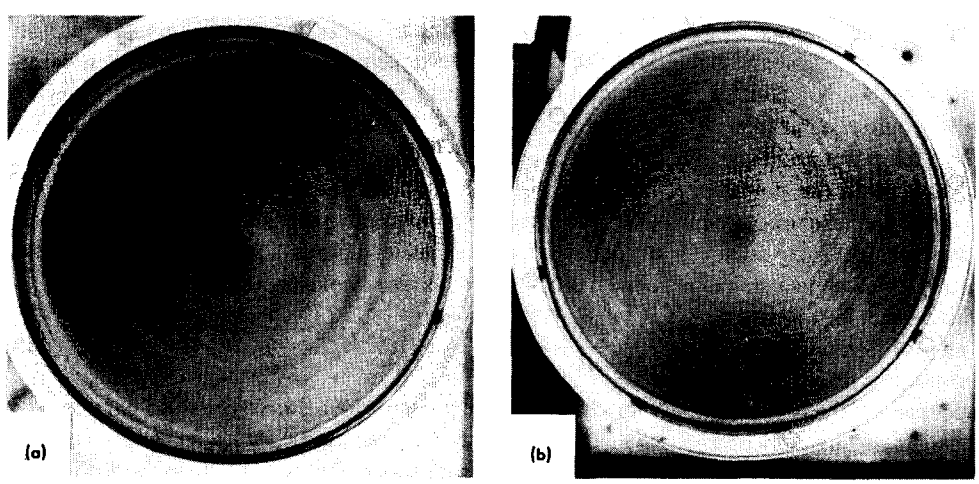

FIG. 4. Waves and the nature of the disk boundary layers at higher initial rotation rates. Clockwise rotation. (a) $\Omega_i = 3.14$ rad/sec, $t = 1.0$ sec, $\Omega_i t = 3.1$ rad; and (b) $\Omega_i = 6.28$ rad/sec, $t = 0.4$ sec, $\Omega_i t = 2.4$ rad.

The motion of the core has to be considered. Asymptotic decay of the core flow during spindown to rest can be represented by $\Omega(t) = \Omega_i [1 + 0.69(2R/H)(\nu\Omega_i/R^2)^{1/2}t]^{-2}$, where Ω is the angular velocity.[10] It follows that the core has slowed down by about 9% by the time of Fig. 2(d). No coupling is observed in the cross-sectional view between the circular waves and the motion of the core. Therefore, it is concluded that the wave phenomenon is a property of the disk boundary layer. The number of observable cycles is limited by the size of the apparatus and the Reynolds number.

Observations made in a Bödewadt-type boundary layer occurring during impulsive spindown to rest in a cylindrical cavity show that a new class of circular waves are excited. These waves occur deep in the boundary layer and move toward the center. At sufficiently high Ekman numbers the well-known waves of type I are also excited along with the circular waves.

[1]Th. v. Kármán, Z. Angew. Math. Mech. **1**, 233 (1921).
[2]U. T. Bödewadt, Z. Angew. Math. Mech. **20**, 241 (1940).
[3]M. H. Rogers and G. N. Lance, J. Fluid Mech. **7**, 617 (1960).
[4]N. Gregory, J. T. Stuart, and W. S. Walker, Phil. Trans. A **248**, 155 (1955).
[5]A. J. Faller, J. Fluid Mech. **15**, 560 (1963).
[6]A. J. Faller and R. E. Kaylor, *Dynamic of Fluids and Plasmas*, edited by S. I. Pai (Academic, New York, 1966), p. 309.
[7]P. R. Tatro and E. L. Mollo-Christensen, J. Fluid Mech. **28**, 531 (1967).
[8]E. R. Benton, J. Fluid Mech. **24**, 781 (1966).
[9]H. P. Greenspan, *The Theory of Rotating Fluids* (Cambridge U. P., Cambridge, 1969).
[10]P. D. Weidman, J. Fluid Mech. **77**, 685 (1976).

A Lagrangian two-time probability density function equation for inhomogeneous turbulent flows

S. B. Pope
Sibley School of Mechanical and Aerospace Engineering, Cornell University, Ithaca, New York 14853

(Received 6 September 1983; accepted 28 September 1983)

An exact equation for the Lagrangian two-time velocity joint probability density function (pdf) is derived from the Navier–Stokes equation. The pdf equation contains as an unknown the conditional expectation of the fluid acceleration. A linear Markov model is proposed which leads to a modeled equation that is consistent both with Kolmogorov's theory in the inertial subrange and with Reynolds-stress models. The dissipation rate is obtained from the joint pdf in a way that is consistent with the modeled dissipation equation. A Monte Carlo method can be used to solve the modeled two-time pdf equation for inhomogeneous turbulent flows.

Several turbulent flow calculations have been reported based on one-point pdf methods.[1–3] In these methods a modeled transport equation is solved for the joint probability density function (pdf) of the three components of velocity $\mathbf{U}(\mathbf{x},t)$ at position $\mathbf{x}$ and time t. This approach has the advantage (compared to Reynolds-stress closures[4,5]) that convective transport appears in closed form and hence gradient-diffusion modeling is avoided.

The one-point joint pdf $f(\mathbf{V};\mathbf{x},t)$ (where V_1, V_2, and V_3 are the independent velocity variables) provides a complete statistical description of the velocity at each point and time, but it contains no joint information at two or more points. Consequently a time or length scale of turbulence cannot be deduced from f and (as with Reynolds-stress closures) scale information must be provided separately. This can be done either explicitly[1–3] or indirectly through the solution of a modeled transport equation for the rate of dissipation ϵ.[4,5] The direct specification of scale information is only possible in simple flows, and the validity and accuracy of the modeled dissipation equation has often been called in question (for example Ref. 6).

Multipoint pdf equations have been derived and modeled[7,8] but solutions have been obtained only for homogeneous isotropic turbulence.[7] The Monte Carlo methods,[9,10] by which the one-point pdf equations can be solved for inhomogeneous flows, cannot be simply extended to multipoint equations.

Here we consider a Lagrangian two-time pdf equation. This pdf contains both time-scale and length-scale information and its transport equation is amenable to solution by a Monte Carlo method. A simple model is proposed that is consistent both with Kolmogorov's theory in the inertial subrange and with Reynolds-stress models.

We consider a constant property turbulent flow (with unity density and viscosity μ) in which the Eulerian velocity $\mathbf{U}(\mathbf{x},t)$ satisfies the Navier–Stokes equation

$$\frac{\partial U_j}{\partial t} + U_i \frac{\partial U_j}{\partial x_i} = \mu \nabla^2 U_j - \frac{\partial p}{\partial x_j}, \tag{1}$$

where $p(\mathbf{x},t)$ is the pressure. At time t the fluid particle at $\mathbf{x}$ has the Lagrangian position $\hat{\mathbf{x}}(t) = \mathbf{x}$ and velocity $\hat{\mathbf{U}}(t) = \mathbf{U}(\mathbf{x},t)$. At an earlier time s ($s < t$) the same fluid parti-

0031-9171/83/123448-03$01.90